Research Project Technical Completion Report

OWRRI Project No. A-030-Oklahoma

HYDRAULICS of MAIN CHANNEL-FLOODPLAIN FLOWS

Charles E. Rice

Assistant Professor of Agricultural Engineering

Oklahoma State University

Period Covered by Research Investigation

July 1, 1971 through June 30, 1974

The work upon which this report is based was supported in part by funds provided by the United States Department of the Interior, Office of Water Resources Research, as authorized under the Water Resources Research Act of 1964.

HYDRAULICS OF MAIN CHANNEL-FLOODPLAIN FLOWS

Objectives And Extent Of Achievement Of The Objectives

The Objectives of the study were:

1. To evaluate qualitatively and quantitavely, from physical model experiments, the effect of floodplain flow on the flow in the main channel.
2. To evaluate the adequacy and accuracy of the commonly used methods to calculate the uniform discharge in combined channels for several variable combinations and to develop an improved method for calculating the uniform discharge.
3. To develop criteria that will enable the researcher or the hydrologist to apply the hydrodynamic equations of unsteady flow to main channel-floodplain flow combinations.

Objective one, the major objective of the project was achieved satisfactorily. Data were obtained relating: the Manning coefficient n to depth of flow for the combined channel for different floodplain to main channel width ratios; the Manning coefficient n to the floodplain to main channel depth ratio for different floodplain to main channel width ratios; the hydraulic radius R to flow depth; the discharge to flow depth; and the channel conveyance to $AR^{2/3}$ ratio. Also, dimensionless parameters involving the quantities pertinent to the study were used and multivariable linear and exponential equations developed to predict the combined channel Manning coefficient.

Objective two was only partially achieved. The first part, that of evaluating some commonly used methods for computing uniform flow in combined channel, was done. An improved method of calculating the uniform flow discharge in combined channels was not achieved.

It was not possible to completely achieve objective three because of limitations in the physical setup. The channel section was so short that a true uniform flow could not be developed for the complete test reach length. There appeared to be some backwater effect at the downstream station of the test reach. Also, there was little attenuation of the flood wave for the short reach length making if difficult to obtain depth differences along the channel reach that were adequate to satisfactorily achieve the objective. However, sufficient data were obtained to check the use of the unsteady flow equations for routing down a combined channel by breaking the combined channel into the floodplain and main channel sections. Data were also obtained to relate the elevations of the main channel and floodplain during the passage of a flood wave through a channel reach.

Equipment

The data were obtained from controlled experiments with a physical system. The system consisted of a combined channel made from galvanized sheet metal for the channel section with plastic or rubber netting used as the surface roughness material; pumping system including two pumps, pipelines, storage sump, settling tank, water meters and stilling well; one-foot H-flumes; piezometer openings which connected to the gage wells equipped with the point gages to measure the water surface elevation in the gage wells, and connected to physiological pressure transducers and Sanborn dual channel recorders to measure unsteady flows; vertical dividers used to separate and permit the measurement of discharge in the individual channel sections; automatic and non-automatic switch boards connected with the control valves. The botton elevations of the channels and gage zeros were found using an engineer's level and point gage.

The Combined Channel

The combined channel system consisted of 2 44-feet long, 18- by 7½-inch steel WF beams on edge which supported the built-up channel section. The combined channel system had a rectangular main channel with horizontal floodplain section. The maximum ratio of the floodplain width to the main channel width was about 7.0 and the ratio of the floodplain depth to the main channel depth varied between zero and about 0.6. The shape and dimensions of the combined channel cross section are presented in Figure 1. The total channel length was about 44-feet with a test reach length of 20-feet near the longitudinal center of the channel. The main channel and the floodplain channel could be divided using a vertical sheet metal wall. The channel slopes were adjusted by using screw jacks under the channel.

Surface Roughness

Because it was expected that the floodplain roughness has a significant effect on the main channel flow, three different artificial roughness were used for the floodplain surface roughness. One of the floodplain surface roughnesses was the same as the main channel roughness but the others were different. Only one roughness was used for the main channel for all of the tests. The surface roughness were simulated using two plastic nettings and one rubber netting.

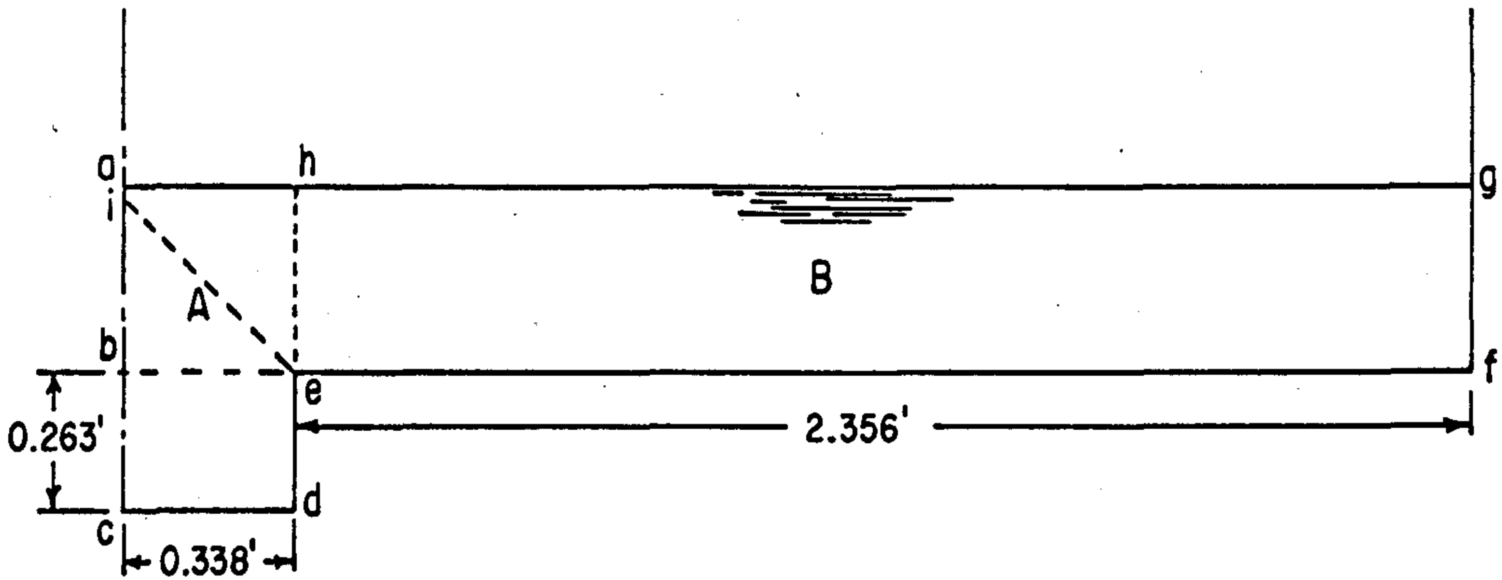

Figure 1 Cross Section and Dimensions of the Tested Combined Channel

Flow Measurement

Both the inflow and outflow of the channel system was measured. The devices used to measure the outflows from both the main channel and the floodplain channel were one-foot H-fumes. Small inflows into the channel were measured with a 2-inch nutating disc totalizing water meter and large discharges, over 100 gallons per minute, were measured with a Sparling meter.

Depth Measuring Equipment

Three depth measuring stations for water surface elevations were located at distances 0+11, 0+21 and 0+31-feet down the channel from the upstream end. At each station one brass plug with hole of about 0.07 in. bore and two brass plugs with holes of about 0.07 in. bore were used as piezometer taps to measure the flow depth in the main channel and the floodplain channel respectively. The brass plugs were set level with the inside botton of the channels. The bottom ends of these piezometers had been counterborded to cut down surface tension and capillary effect. Plastic tubing was used to connect the piezometers from each station to the stilling wells or pressure transducers.

Procedure

Steady Flow Tests

The test schedule involved two major phases: those tests with the dividers, and those without the dividers to separate the flood plain channel and the main channel. Each part of the schedule used three different roughnesses for the tests, and at each roughness five different slopes, 0.0008, 0.0013, 0.0018, 0.0025 and 0.0033 were used. For each slope 19 different discharges were run including the base flow. At each test, the depths of flow in the main channel and the flood plain channel at each station were observed.

At a particular slope and roughness, the water was pumped from the storage tank. Five to ten minutes were allowed for the flow to attain the equilibrium condition. After an equilibrium condition, depth measurements were made using the point gages, and discharge measurements were made by measuring the head of flow in the flumes and using the calibration curves.

The next slope was set and tested. This was repeated until all five of the slopes had been tested. After all five slopes at one roughness was tested, the next step was to put the dividers on to separate the floodplain channel and the main channel. The joints between the dividers and the bottom of the channel were sealed. Tests were then conducted for the five slopes as previously. Next, the second, and then third roughness conditions were tested.

During the tests, the regime and flow conditions were carefully observed and the temperature of water was recorded. From measurements taken, the cross-sectional area, the wetted perimeter, and the hydraulic radius for each run were determined. The values of roughness coefficient were calculated between stations and the average value of the roughness coefficient for the channel was determined.

Unsteady Flow Tests

The flood waves introduced into the channel were generated using a manifold made up of 18 adjustable valves equipped with electrical solenoids to open and close the valves. The solenoids were activated with an 18 circuit, gear driven, timer. A gear on the timer could be changed to permit different time intervals for opening and closing the valves. This permitted different time bases for the inflow hydrographs with the same peak flow.

For a test, a base flow was set and allowed to stabilize. The pressure transducers and Sanborn recorders were then calibrated using the point gage readings for the steady base flow. The timer was then activated causing the valves to open and close generating the hydrograph at the upstream end of the channel. After the flood wave had moved through the test reach and the system had stabilized with base flow conditions, readings were again taken with the point gages.

Results

Hydraulic Radius Computation

In computing the discharge versus normal depth relationship for the combined channel, it became evident that the hydraulic radius as ordinarily used in the regular channel could not be applied to the entire cross section. The error in computation of discharge based on the hydraulic radius of the entire cross section was large in the portion immediately above bank-full stage, and decreased as the overbank flow depth increased. The discharge computed by this method was generally less than the actual discharge. In the range of depth just above bank full, the flow began to cover the floodplain channel and the wetted perimeter increased very rapidly while the total area increased very little resulting in a decrease in the computed hydraulic radius, velocity and discharge. Several methods have been suggested to obtain a reasonable hydraulic radius. A comparison of computed and observed values of discharge has been made by Posey (1). Each method gave good results for a certain range of flow depths, but no particular method gave good results for all of the depths of flow.

The method used to compute the mean hydraulic radius in this investigation was developed from one suggested by Posey. For this method, the main channel and overbank area and wetted perimeters are computed separately, then added together. The division was along the line ch, Figure 1. The main channel area A, and its wetted perimeter was from the section bcde. The portion ab was not included in the wetted perimeter because the line abc was considered to be the separating line of the symmetrical channel. So, only the portion bc was included in the wetted perimeter. The overbank area and wetted perimeter were B and efg respectively. The line eh was not included in the portion of wetted perimeter in the main channel and floodplain channel because the flow in the main channel and floodplain channel were not considered to be retarded by the shear on the plain eh. The average hydraulic radius of the entire cross section was then computed by dividing the total area by the wetted perimeter of the main channel and the overbank channel as shown:

$$R_{av} = \frac{A + B}{bcde + efg} \qquad (1)$$

Manning Coefficient

The Manning Coefficients were computed using the Manning equation with the friction slope computed using the gradually varied flow procedure. The variation of the Manning n with depth for one condition of the combined channel is presented in Figure 2. The average n value decreased as the depth of flow increased until overbank flow occurred. Then it increased as the depth of flow increased, to a point at which it was almost constant or slightly decreasing. The data on Figure 2 are for roughness condition one, main channel and floodplain roughness material the same. The n versus depth relationships for roughness conditions two and three are similar but the overbank n values are a little larger.

Figure 3 presents the combined channel Manning Coefficient versus depth for different floodplain to main channel width ratios. These data show that as the floodplain width increases relative to the main channel width, the combined channel n value increases. This suggests that the floodplain flow has a significant retarding effect on the main channel flow.

Figure 4 presents the main channel and floodplain Manning n values as a function of the floodplain to main channel depth ratio . These results show a large variation in the floodplain n values with depth and very little variation of the main channel n values. In general, the smaller the floodplain width, relative to the main channel width, the less difference between the main channel and floodplain n values. The reason the floodplain n values, at the floodplain to main channel width ratio of 1.32,

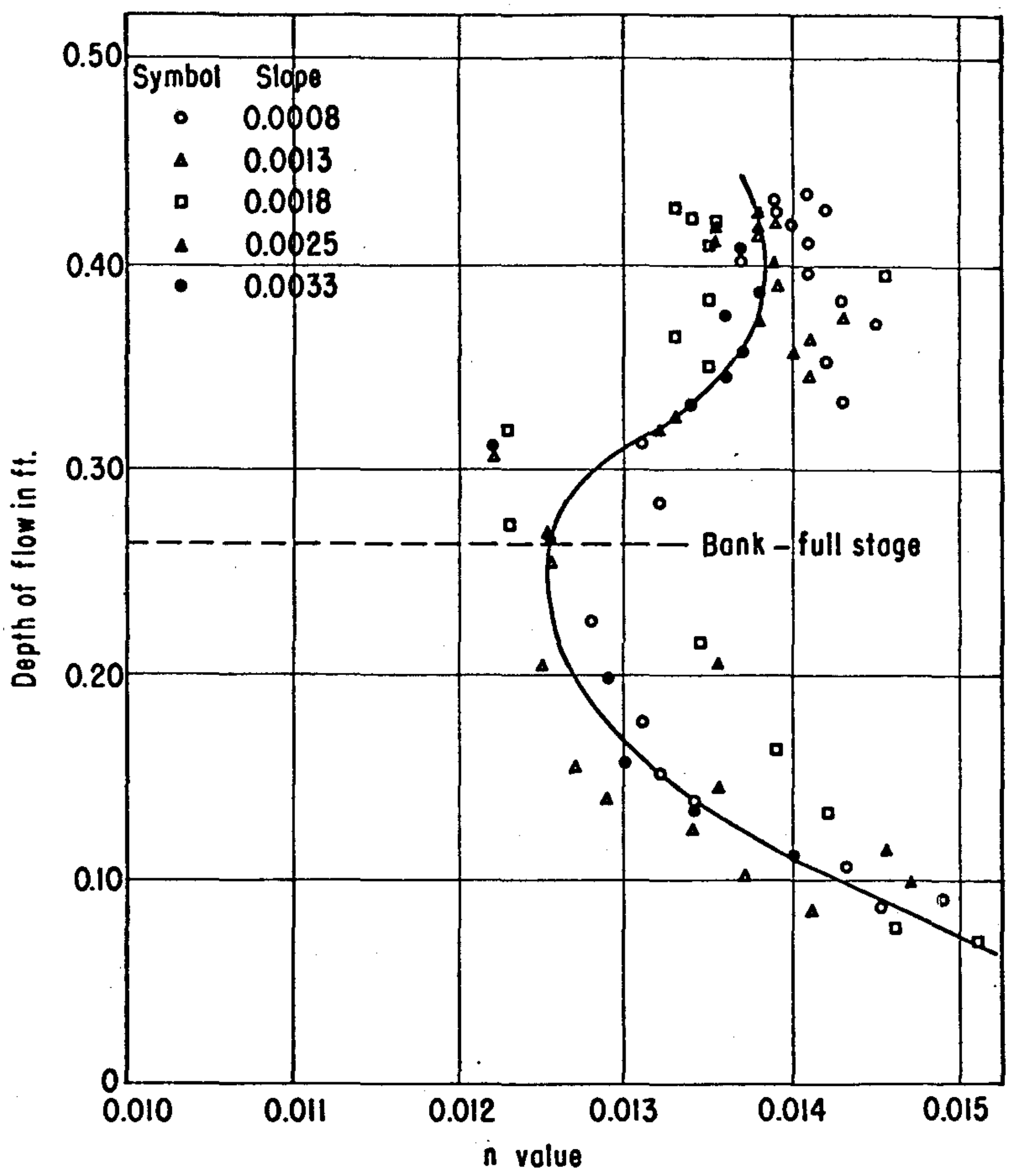

Figure 2 Variations of the n Value with the Depth of Flow with Roughness Number 1; the floodplain to main channel width ratio is 6.97.

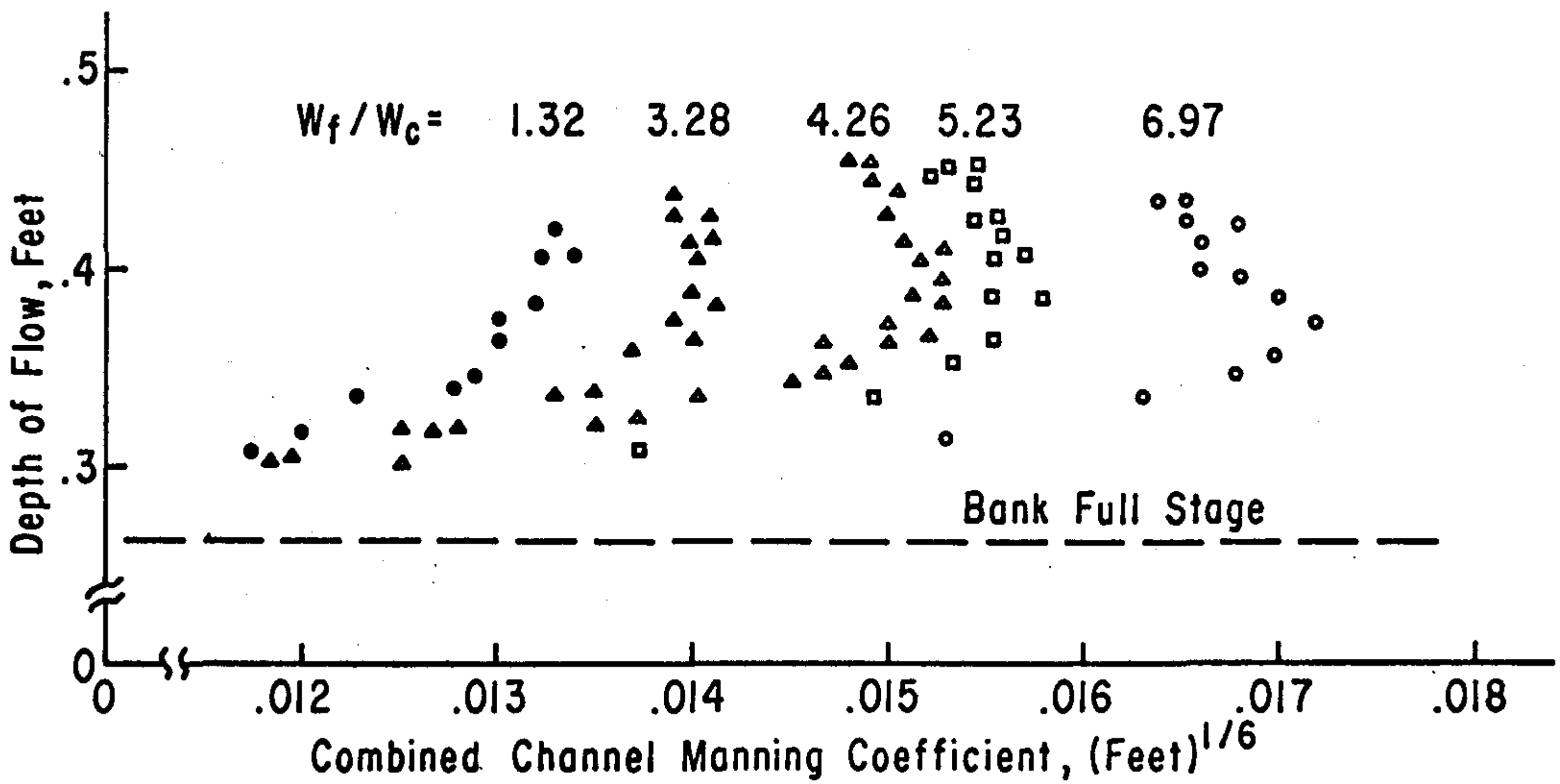

Figure 3 Variation of the combined channel Manning coefficient with flow depth at different floodplain to main channel width ratios for roughness condition three.

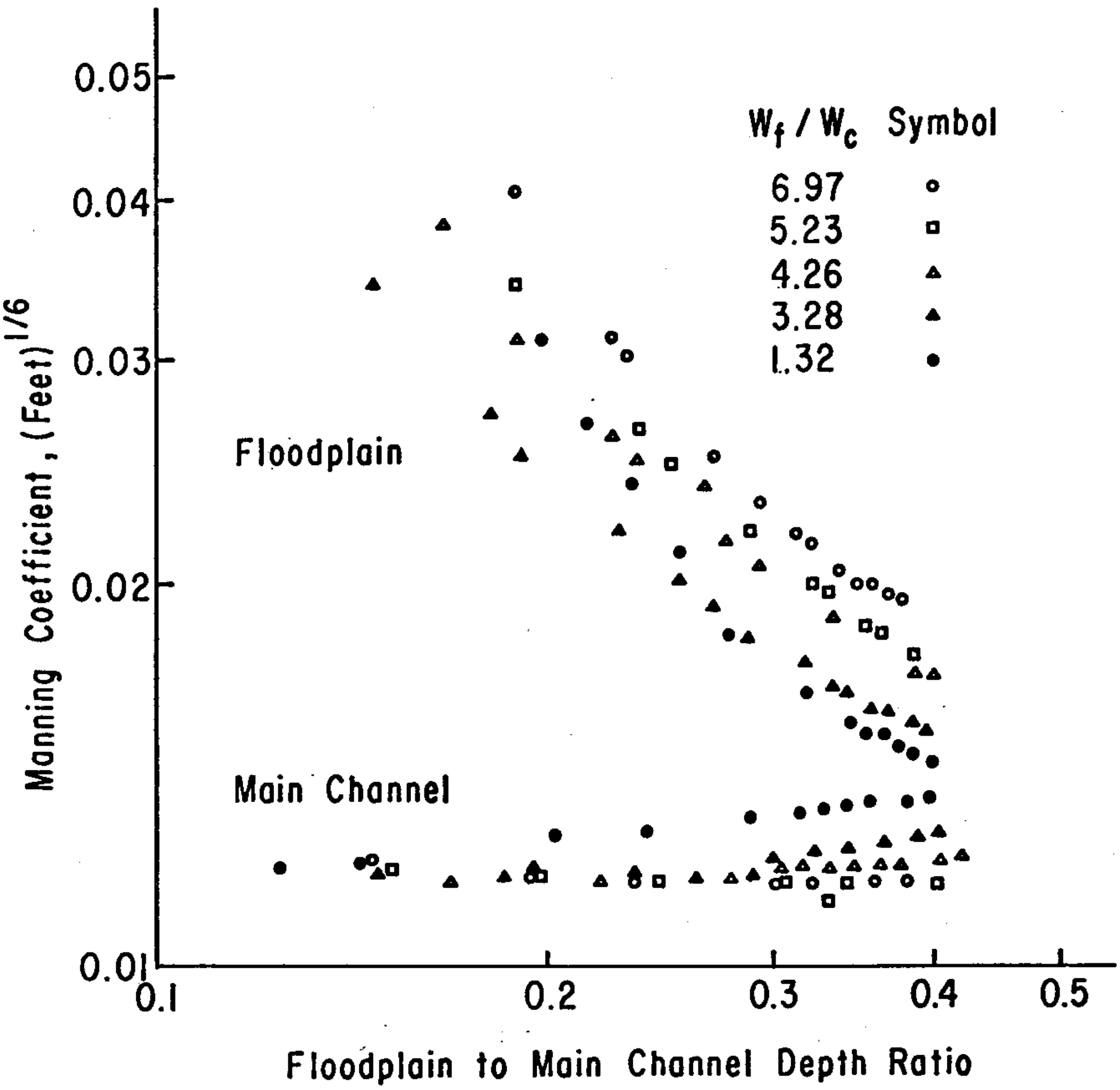

Figure 4 Variation of main channel and floodplain Manning coefficients with depth at different floodplain to main channel depth ratios for roughness condition three. Channel slope varies between 0.0020 and 0.0022.

crosses over the other n values is not known for sure, but it may be due to the influence of the wall roughness on the flow for the narrower floodplain width. In the analysis, the floodplain vertical wall was assumed frictionless and this assumption becomes less correct as the floodplain width decreases.

Results With and Without Divider

For the steady flow conditions, tests were run with the channel cross section acdefg, Figure 1, and also with a vertical divider at eh, Figure 1, to separate the combined channel into the main channel and floodplain sections. Figure 5 presents the variations of mean hydraulic radius R with depth of flow and Figure 6 presents the discharge versus depth with and without divider

When the flow depth did not exceed the main channel stage, the hydraulic radius increased as the depth increased. As the depth just exceeded the main channel depth, the hydraulic radius decreased significantly and then increased as the depth increased. The water surface elevations in the main channel and floodplain without the divider were almost the same.

With the divider, the water surface elevations in the main channel were lower than in the floodplain channel. The hydraulic radius and the wetted perimeter of the floodplain were greater with the divider than without the divider for the same depth of flow on the main channel. Thus, the higher value of hydraulic radius as shown in Figure 5 and the higher discharges as shown in Figure 6.

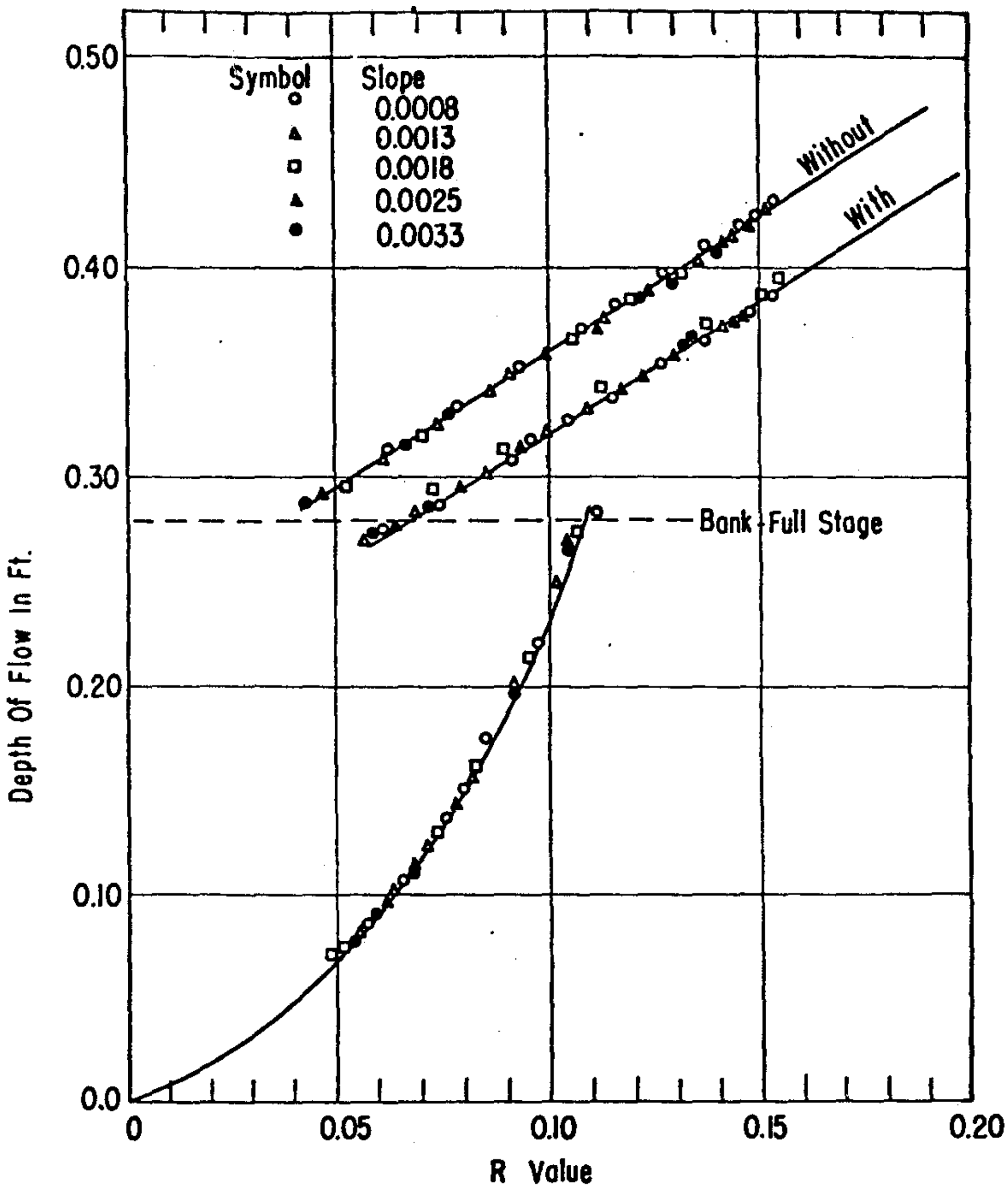

Figure 5 Variations of the Mean Hydraulic Radius R With the Depth of Flow, (From Roughness Number 1) with and without Divider

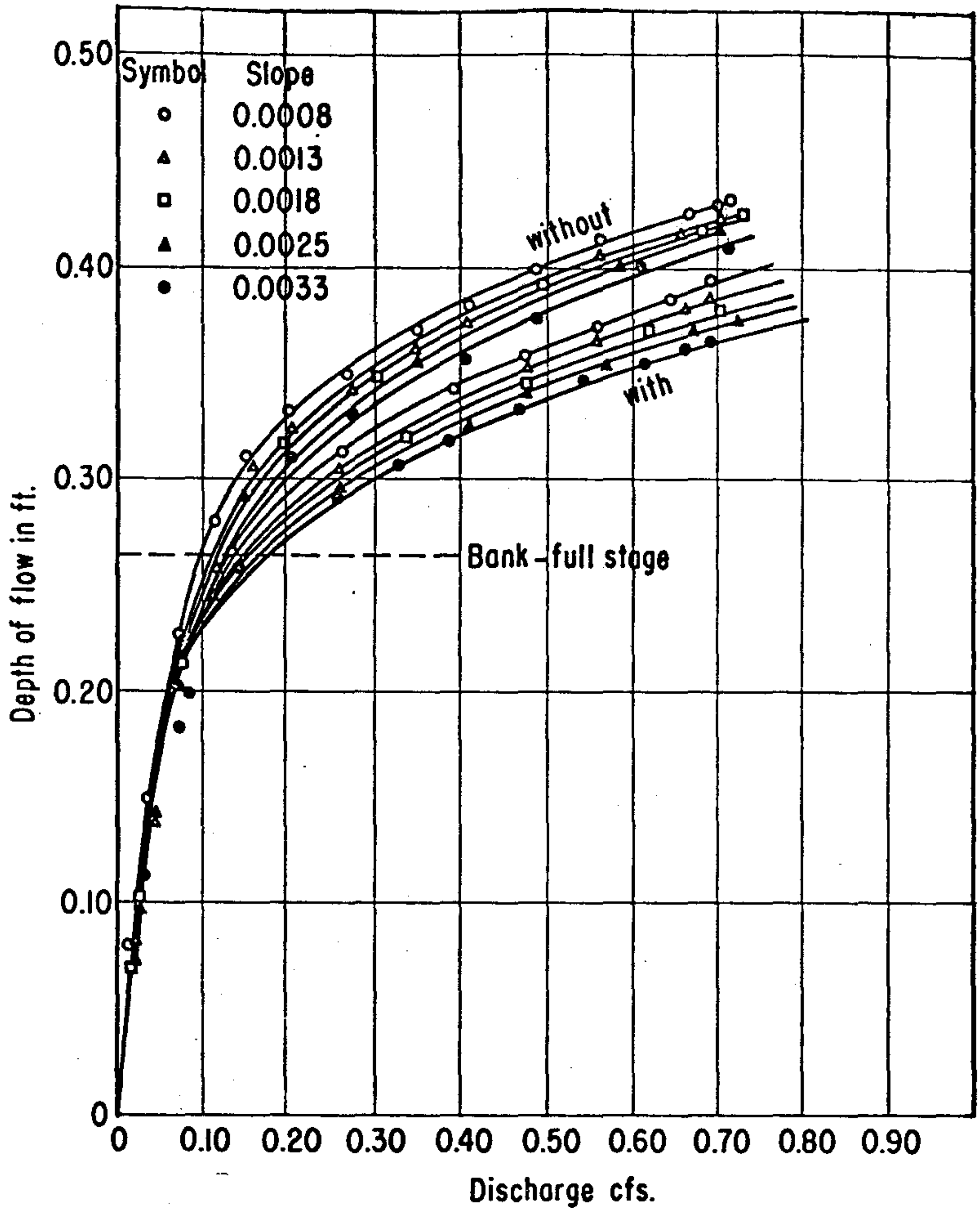

Figure 6 Depth of Flow Versus Normal Discharge, (From Roughness Number 1) With and Without Divider

Channel Conveyance

Figure 7 presents the channel conveyance $Q/\sqrt{S}$ as a function of $AR^{2/3}$ for the combined channel without the divider. These data show that in the portion with main channel flow only, all flow conditions give the same equation. The line passes through the origin with the slope equal to 1.49/n, giving an average value of 0.0125 for the Manning Coefficient for the main channel. For the floodplain flows, the lines do not pass through the origin and each has different intercept and slope. This indicates that for flow computations in a main channel floodplain combination, the Manning equation cannot apply directly. The Manning Coefficient for the combined channel reflects not only the effect of boundary roughness and slope, but also channel geometry.

Dimensional Analysis

Dimensional analysis (2) was used to form dimensionless parameters from the quantities thought pertinent to the prediction of the Manning Coefficient for the combined channel. The list of pertinent quantities used are presented in Table I and the functional relationship for the dimensionless parameters formed is:

$$\left(\frac{n}{R^{1/6}}, \frac{n_c}{R^{1/6}}, \frac{n_f}{R^{1/6}}, \frac{B_c}{R}, \frac{B_f}{R}, S, \frac{V}{\sqrt{gR}}, \frac{VR}{\gamma}\right) = 0 \qquad (2)$$

Multivariable linear and exponential response surfaces of the forms in equations (3) and (4) were fit to the observed data.

Linear form: $$P_1 = C_1 + C_2P_2 + C_3P_3 + C_4P_4 + C_5P_5 + C_6P_6 + C_7P_7 + C_8P_8 \qquad (3)$$

Exponential form: $$P_1 = B_1 P_2^{B_2} P_3^{B_3} P_4^{B_4} P_5^{B_5} P_6^{B_6} P_7^{B_7} P_8^{B_8} \qquad (4)$$

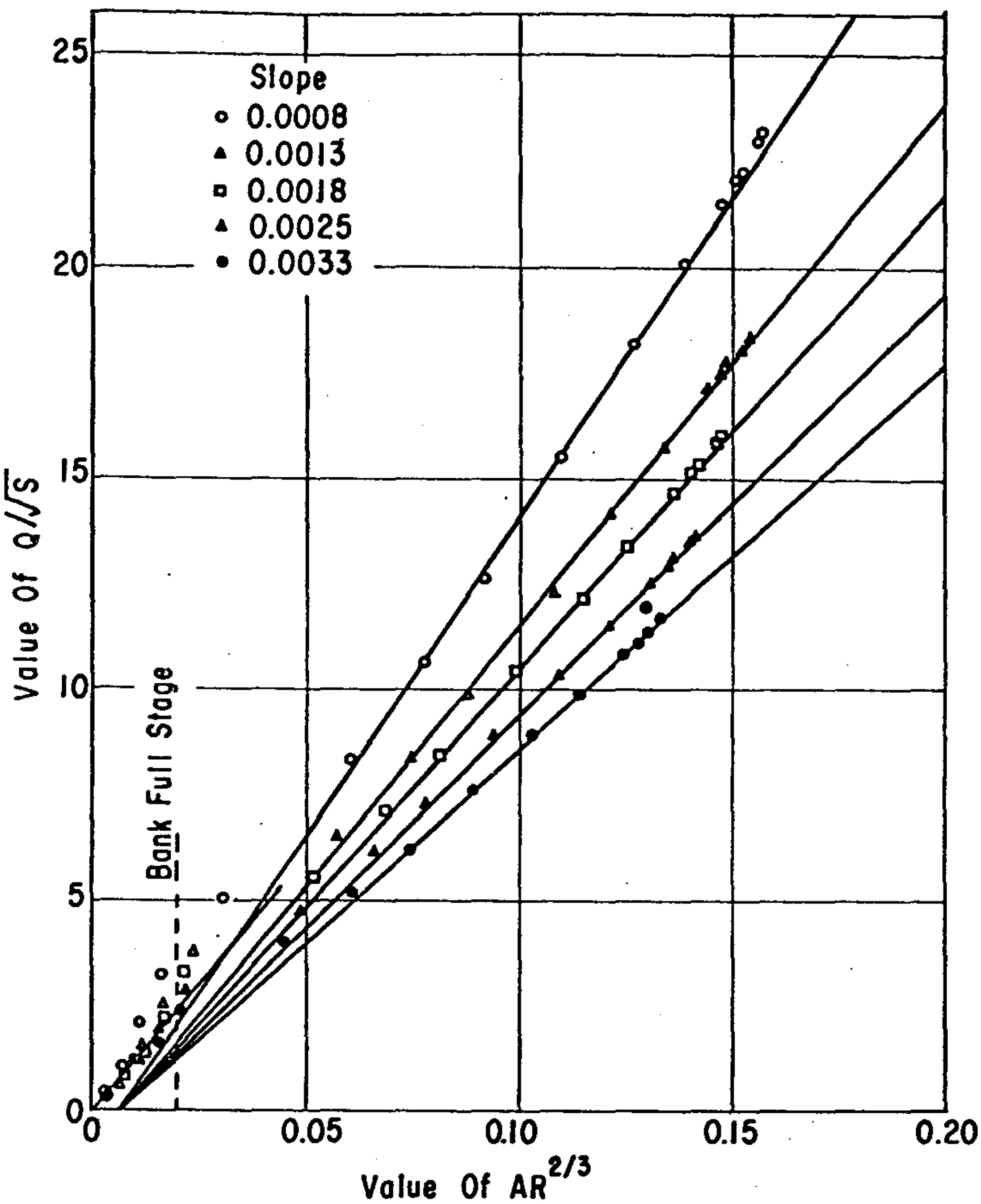

Figure 7 Conveyance Versus $AR^{2/3}$ For Channel Without Divider And Roughness Number 3

TABLE I

PERTINENT QUANTITIES

Number	Symbol	Quantity	Unit	Dimensions
1.	n	Roughness coefficient of the combined channel	ft.$^{1/6}$	$L^{1/6}$
2.	n_c	Roughness coefficient of the main channel	ft.$^{1/6}$	$L^{1/6}$
3.	n_f	Roughness coefficient of the flood plain channel	ft.$^{1/6}$	$L^{1/6}$
4.	R	Mean hydraulic radius	ft.	L
5.	V	Mean velocity of flow	ft./sec.	LT^{-1}
6.	B_c	Bed width of the main channel	ft.	L.
7.	B_f	Bed width of the flood plain channel	ft.	L.
8.	S	Slope of the channel	—	—
9.	g	Acceleration of gravity	ft./sec.^{2}	LT^{-2}
10.	ν	Kinematic viscosity of water	ft.^{2}/sec.	L^2T^{-1}

Where

$$P_1 = n/R^{1/6} \qquad P_5 = {}^{B}f/_{R}$$

$$P_2 = {}^{n}c/_{R}{}^{1/6} \qquad P_6 = S$$

$$P_3 = {}^{n}f/_{R}{}^{1/6} \qquad P_7 = V/\sqrt{gR}$$

$$P_4 = {}^{B}c/_{R} \qquad P_8 = {}^{V}R/_{\gamma}$$

The coefficients for equations (3) and (4) and the correlation coefficients and standard deviations for the observed data versus that data found using the fitted equations are presented in Tables II and III.

Uniform Flow Computations

The methods of mean hydraulic radius and uniform flow computation suggested by Posey (1) are applied to the combined channel as shown in Figure 1.

Method 1. The whole area A+B is divided by the entire wetted perimeter abcdefg to obtain the mean hydraulic radius. Then the average velocity is computed and multiplied by the total area A+B to obtain the total discharge.

Method 2. The main channel and over-bank discharge are computed separately, then added together. The division line is along the line eh. The main channel area A and its wetted perimeter is considered to be abcdeh. The over-bank area B and its wetted perimeter is efg.

Method 3. This method is the same as method 2, except that the portion ab and eh are not considered in part of the main channel wetted perimeter.

TABLE II

EXPERIMENTAL COEFFICIENTS, CORRELATION COEFFICIENT (R), AND STANDARD DEVIATION (S) OF MULTIVARIABLE LINEAR EQUATIONS FOR COMPUTING DIMENSIONLESS RESISTANCE COEFFICIENTS*

FL NO	FOR SLOPE	WITH DIVIDER	C1	C2	C3	C4	C5	C6	C7	C8	CORR COE R	STAN DEV S
			EXPERIMENTAL COEFFICIENTS									
1	0.0008	NOT	0.879246	1.166901	-0.015771	0.007477	-0.002570	148.917900	-1.785103	0.000007	0.999948	0.003939
2	0.0013	NOT	0.643481	0.802633	-0.036833	0.018648	0.005257	341.449900	-1.926808	0.000008	0.999900	0.005170
3	0.0018	NOT	0.710352	1.049038	-0.311406	0.134957	0.004124	159.000000	-2.365445	0.000017	0.999796	0.007438
4	0.0025	NOT	1.143188	0.568497	-0.089700	0.500423	-0.049776	68.812500	-2.434026	0.000012	0.999796	0.008069
5	0.0033	NOT	3.691081	0.607558	0.122868	0.401798	-0.057522	-756.890600	-1.310227	-0.000003	0.999934	0.004556
6	0.0008	WITH	3.396173	0.679974	-0.553274	0.263771	0.003027	-1911.000000	-3.720860	0.000019	0.999860	0.007400
7	0.0013	WITH	-2.676884	1.544484	-0.457545	0.545293	-0.086446	2513.941000	-0.688645	-0.000004	0.999846	0.007502
8	0.0018	WITH	-0.001372	0.386961	-0.254557	0.507661	-0.034404	605.375000	-2.053646	0.000009	0.999972	0.003181
9	0.0025	WITH	1.730001	-0.001475	0.043282	0.199247	0.003321	142.250000	-3.125345	0.000010	0.999640	0.007230
10	0.0033	WITH	-1.382211	0.736000	-0.022095	0.316187	0.009588	990.750000	-2.665530	0.000010	0.999829	0.006802
11	0.0008	NOT	1.326319	0.347587	-0.009948	0.224331	-0.005167	-729.125000	-1.552013	0.000007	0.999960	0.003129
12	0.0013	NOT	0.740077	0.087203	-0.018651	-0.111716	0.051923	-51.769530	-1.398622	0.000006	0.999891	0.005169
13	0.0018	NOT	1.286341	0.634284	-0.000207	1.135244	-0.149746	-39.515620	-2.157913	0.000005	0.999941	0.004685
14	0.0025	NOT	-1.352446	1.309577	0.002437	0.018392	-0.003706	1174.312000	-2.918877	0.000012	0.999968	0.002973
15	0.0033	NOT	-1.568435	-1.349301	0.038849	-1.503990	0.296060	926.812500	-2.492956	0.000011	0.999660	0.009551
16	0.0008	WITH	-0.313538	1.552643	0.242996	-0.383902	0.034804	2174.875000	-2.824619	0.000010	0.999786	0.009278
17	0.0013	WITH	1.469060	0.654010	-0.922734	-0.328781	0.114664	-88.193840	-2.737796	0.000010	0.999938	0.004687
18	0.0018	WITH	1.325638	0.343906	-0.536116	0.413172	0.003561	-184.484300	-1.974851	0.000007	0.999903	0.006198
19	0.0025	WITH	-0.035030	0.516476	-0.184638	0.120068	0.016078	668.375000	-2.907321	0.000011	0.999981	0.002540
20	0.0033	WITH	16.720850	3.582287	-0.075540	3.574286	-0.589185	-4580.253000	-2.312795	-0.000002	0.999162	0.016952
21	0.0008	NOT	-1.083599	1.497505	-0.034742	-0.439008	0.064541	1823.367000	-0.850479	0.000002	0.999980	0.002543
22	0.0013	NOT	0.428312	1.328229	0.064725	-0.081177	-0.002174	99.392590	-0.430847	-0.000007	0.999805	0.005555
23	0.0018	NOT	0.741472	0.800856	-0.038478	0.159079	-0.002923	231.054600	-2.462590	0.000014	0.999940	0.003389
24	0.0025	NOT	-3.092426	1.295564	-0.322103	-0.457519	0.101479	1124.064000	-0.143781	0.000003	0.999870	0.005295
25	0.0033	NOT	-1.816415	-2.507277	-0.152246	-0.772396	0.250672	594.586900	-0.765559	0.000006	0.999784	0.007218
26	0.0008	WITH	-4.608174	2.028477	-0.350143	-1.914540	0.273913	6895.500000	-1.865971	0.000004	0.999925	0.005372
27	0.0013	WITH	1.554242	0.271433	-0.190999	-0.194703	0.072343	-69.562500	-2.901048	0.000013	0.999921	0.005006
28	0.0018	WITH	1.267805	0.664443	-0.126093	0.180123	0.002657	-8.546875	-2.330255	0.000008	0.999965	0.003688
29	0.0025	WITH	-0.999416	0.846382	-0.140057	0.357881	-0.025476	844.492100	-2.091287	0.000009	0.999955	0.004174
30	0.0033	WITH	-2.304094	-0.216406	-0.053414	0.095642	0.033358	1145.757000	-2.270752	0.000010	0.999959	0.003590

* P1 = C1 + C2*P2 + C3*P3 + C4*P4 + C5*P5 + C6*P6 + C7*P7 + C8*P8

TABLE III

EXPERIMENTAL COEFFICIENTS, CORRELATION COEFFICIENT (R), AND STANDARD DEVIATION (S) OF MULTIVARIABLE EXPONENTIAL EQUATIONS FOR COMPUTING DIMENSIONLESS RESISTANCE COEFFICIENTS*

EG NC	FOR SLOPE	WITH DIVIDER	EXPERIMENTAL COEFFICIENTS B1	B2	B3	B4	B5	B6	B7	B8	CORR COE R	STAN DEV S
1	0.0008	NOT	1.041500	0.605106	0.081721	-0.231253	0.062049	0.034992	-1.180925	-0.044527	0.999909	0.005211
2	0.0013	NOT	0.892283	0.709429	-0.006572	-0.114612	0.082135	0.016290	-0.977581	-0.046786	0.999934	0.004202
3	0.0018	NOT	0.019704	0.590390	0.089367	0.021113	0.940620	0.856295	-1.453923	0.597666	0.999886	0.005566
4	0.0025	NOT	0.816368	0.796222	-0.171663	0.152340	0.037567	0.025494	-0.900410	-0.035610	0.999906	0.005461
5	0.0033	NOT	2.263631	0.634835	0.002423	0.261033	-0.343883	-0.244552	-0.757357	-0.184468	0.999948	0.004054
6	0.0008	WITH	0.805693	0.676456	-0.377658	0.302258	0.084866	0.034659	-0.939403	-0.062091	0.999970	0.00341[illegible]
7	0.0013	WITH	577.166200	2.495784	0.950767	-6.651182	-0.263757	-4.279695	0.847892	-2.666107	0.998467	0.02367[illegible]
8	0.0018	WITH	0.000002	0.442990	-0.160495	-1.039927	2.982339	0.724372	-1.834693	0.955503	0.999618	0.008160
9	0.0025	WITH	2.056216	0.393962	-0.009731	0.268496	-0.232610	-0.232552	-0.747966	-0.205590	0.999915	0.005278
10	0.0033	WITH	1.032119	0.384246	0.150910	0.201674	-0.101885	0.016867	-0.938202	-0.010963	0.999898	0.005258
11	0.0008	NOT	0.854020	0.369482	0.038338	0.246575	-0.119481	-0.092421	-0.724745	-0.102399	0.999971	0.002677
12	0.0013	NOT	0.593631	0.416840	-0.007325	0.568102	-0.012360	0.259597	-0.818463	0.120892	0.999956	0.003280
13	0.0018	NOT	0.905211	0.609970	0.035906	0.026497	-0.011945	0.011282	-0.969311	-0.037932	0.999919	0.005480
14	0.0025	NOT	0.169043	0.487921	0.084132	-0.068985	0.597396	0.488084	-1.321730	0.242062	0.999957	0.003455
15	0.0033	NOT	5.186975	0.171779	0.014569	1.517877	-1.078585	-0.149509	-0.778939	-0.138108	0.999861	0.005638
16	0.0008	WITH	0.785210	0.775923	0.090702	-0.375878	0.386194	0.232070	-0.933044	0.087322	0.999893	0.006569
17	0.0013	WITH	0.242024	1.048829	0.927710	-5.434586	2.304703	-1.848865	0.179698	-1.210872	0.999705	0.010196
18	0.0018	WITH	0.991146	0.548005	0.064212	-0.138581	0.098551	-0.110407	-0.789516	-0.117106	0.999928	0.005349
19	0.0025	WITH	1.217865	0.547091	-0.062859	0.157678	0.002786	-0.026528	-0.814607	-0.085646	0.999976	0.002891
20	0.0033	WITH	1.019124	0.453429	-0.264497	0.481618	-0.012018	-0.082975	-0.645503	-0.122151	0.999983	0.002398
21	0.0008	NOT	0.859163	1.137202	-0.148264	0.047693	0.022817	-0.010809	-0.555348	0.003389	0.999980	0.002540
22	0.0013	NOT	1.418965	1.028221	-0.122290	-0.275238	0.107771	-0.255295	-0.228868	-0.197532	0.999661	0.007309
23	0.0018	NOT	1.137702	0.641165	0.141924	-0.167556	-0.037419	-0.006871	-1.064872	-0.042945	0.999923	0.003834
24	0.0025	NOT	0.903548	0.910543	-0.307060	0.171033	0.162085	-0.050212	-0.601706	-0.095776	0.999846	0.005752
25	0.0033	NOT	0.000000	-2.341867	-0.210020	-1.192417	7.498880	2.932033	-2.225137	1.751178	0.999685	0.008712
26	0.0008	WITH	0.950480	1.234637	-0.265524	-0.119617	0.041074	0.002247	-0.839984	0.000391	0.999826	0.008157
27	0.0013	WITH	4.660919	0.553249	-0.052475	-0.113460	-0.418715	-0.702267	-0.411397	-0.517856	0.999933	0.004631
28	0.0018	WITH	3.652844	0.438883	-0.006628	-0.231137	-0.201077	-0.640742	-0.445672	-0.488125	0.999966	0.003658
29	0.0025	WITH	1.599536	0.322409	-0.110848	0.131917	0.103177	-0.173940	-0.613999	-0.230879	0.999959	0.003950
30	0.0033	WITH	0.343946	0.095645	-0.119484	1.052122	0.221704	0.733697	-1.106597	0.306086	0.999879	0.006168

* P1 = B1*(P2**B2)*(P3**B3)*(P4**B4)*(P5**B5)*(P6**B6)*(P7**B7)*(P8**B8)

Method 4. The cross section area is divided into parts by an imaginary line bisecting the re-entrant angle at c. The hydraulic radius of each part is computed separately, including only solid boundaries as wetted perimeter. The average hydraulic radius for the entire section is then computed by weighting the hydraulic radius of each part with its area as

$$R_{av} = \frac{A^2/bcde + B^2/efg}{A+B} \tag{5}$$

Comparison of Methods

Comparisons are made from one of the experiments. Table V shows the comparison of the discharges computed by the four methods. The roughness coefficients used for method 1, and method 4 are the average roughness coefficients for the entire cross section computed using the Manning equation. The roughness coefficients used for method 2 and method 3 are the average roughness coefficients computed from the main channel and flood plain channel by using the Manning equation on each section separately.

From Table VI, the roughness coefficients used for each method are computed using the Manning equation for each flow depth. Method 1 and method 4 used the roughness coefficients computed from the entire section for each flow depth, but for method 2 and method 3, the roughness coefficients used are computed from the main channel and from the floodplain channel separately.

The slopes used for computing these discharges are the friction slopes computed assuming gradually varied flow for each flow depth. In real-life, the slope used in the Manning equation is the bottom slope because it is easy to find. For the gradually varied flow condition, these two slopes are almost identical and for the general

TABLE V

COMPARISON OF COMPUTED AND OBSERVED DISCHARGE FROM EXPERIMENT NUMBER 2 USING AVERAGE ROUGHNESS COEFFICIENT

Y ft.	Discharge and discrepancy, computed by								Obs. disch cfs.	Min. dis %
	1		2		3		4			
	Disch	Dis	Disch	Dis	Disch	Dis	Disch	Dis		
0.308	0.144	-5.88	0.168	+10.00	0.177	+15.49	0.171	+11.43	0.153	-5.88
0.325	0.199	-1.68	0.209	+3.36	0.221	+9.40	0.284	+40.69	0.202	-1.68
0.345	0.287	+4.81	0.276	+0.65	0.294	+7.18	0.465	+64.51	0.274	+0.65
0.362	0.359	+3.16	0.337	-3.27	0.360	+3.39	0.625	+79.62	0.348	+3.16
0.374	0.425	+4.91	0.374	-7.70	0.401	-1.03	0.770	+90.09	0.405	-1.03
0.389	0.499	+1.94	0.438	-10.57	0.470	-4.00	0.942	+92.53	0.489	+1.94
0.402	0.540	-4.34	0.495	-12.25	0.533	-5.58	1.100	+95.05	0.564	-4.34
0.413	0.640	+1.12	0.551	-12.98	0.593	-6.39	1.274	+101.20	0.633	+1.12
0.417	0.662	+0.36	0.573	-13.13	0.618	-6.42	1.328	+101.13	0.660	+0.36
0.420	0.680	+1.44	0.588	-12.34	0.633	-5.53	1.370	+104.37	0.670	+1.44
0.424	0.702	+0.02	0.606	-13.71	0.653	-7.00	1.426	+103.06	0.702	+0.02
0.425	0.709	-0.21	0.610	-13.98	0.658	-7.30	1.440	+102.83	0.710	-0.21

TABLE VI

COMPARISON OF COMPUTED AND OBSERVED DISCHARGE FROM EXPERIMENT NUMBER 2 USING ROUGHNESS COEFFICIENT FOR EACH FLOW DEPTH

Y ft.	Discharge and discrepancy, computed by								Obs. disch cfs.	Min. dis %
	1		2		3		4			
	Disch	Dis	Disch	Dis	Disch	Dis	Disch	Dis		
0.308	0.163	+6.47	0.151	-1.56	0.159	+3.98	0.193	+ 26.01	0.153	-1.56
0.325	0.206	+2.02	0.194	-4.15	0.206	+2.12	0.295	+ 45.94	0.202	+2.02
0.345	0.281	+2.59	0.266	-3.10	0.283	+3.43	0.455	+ 66.20	0.274	+2.59
0.362	0.351	+0.97	0.340	-2.38	0.363	+4.28	0.612	+ 75.77	0.348	+0.97
0.374	0.410	+1.25	0.388	-4.24	0.415	+2.41	0.743	+ 83.45	0.405	+1.25
0.389	0.495	+1.20	0.471	-3.70	0.503	+2.90	0.935	+ 91.14	0.489	+1.20
0.402	0.536	-5.01	0.533	-5.56	0.570	+1.09	1.092	+ 93.65	0.564	+1.09
0.413	0.640	+1.12	0.612	-3.34	0.653	+3.19	1.274	+101.20	0.633	+1.12
0.417	0.658	-0.36	0.638	-3.27	0.682	+3.33	1.318	+ 99.69	0.660	-0.36
0.420	0.675	+0.73	0.649	-3.20	0.693	+3.47	1.360	+102.91	0.670	+0.73
0.424	0.697	-0.68	0.673	-4.17	0.719	+2.43	1.415	+101.59	0.702	-0.68
0.425	0.709	-0.21	0.688	-3.08	0.735	+3.49	1.440	+102.83	0.710	-0.21

case, the bottom slope of the channel is known but the friction slope is not.

The results show that method 1 from Table V and Table VI give better results than the other methods. One method that gives reasonable but slightly greater differences is method 3. For the range of depths from the beginning of overbank flow, method 2 gives better results than method 3. Outside of this range method 3 is preferred. Method 4 does not give any reasonable results because of the computed value of mean hydraulic radius by this method is too high in almost every case. This method is not recommended to compute the discharge in combined channels. The method that gives the best result is method 1, and is suggested to use for computing the discharge in combined channel. The very important thing is the method used to estimate the mean or average roughness coefficient for the entire cross section.

These studies show that the method of estimating the average roughness coefficients of the combined channel is one of the problems to be considered, as well as the method of calculating the mean hydraulic radius, in computing discharge in combined channel systems.

Unsteady Flow

The forward and backward characteristic equations of the unsteady flow equations were used to route flood waves through the test channel reach. An explicit finite difference method using a centered difference scheme was used to solve the equations.

In routing the flood waves it was assumed that the transverse water surface at any location along the channel was horizontal. The channel was broken into the main channel and floodplain portions and routed by sections applying the appropriate Manning Coefficient to each section. Some approaches assume that the transverse water surface is not horizontal and that the overbank section provides storage, with very little discharge, on the rising stage and contributes this storage back to the main channel on the recession.

Figure 8 presents data, typical of all test results, showing the elevations of the main channel and floodplain at three stations of the test reach length. These data show that except at the very shallow depths, there is no difference in elevation between the main channel and the floodplain. Also, visual observations during the unsteady flow tests showed discharge on the floodplain at all times once the overbank elevation was exceeded. Thus, for the conditions of these tests, the assumption of a horizontal transverse water surface appears justified. In situations where there is a larger difference between the main channel and floodplain roughness, this may not be justified.

Figure 9 presents a plotting of depth hydrographs for one test condition. From these data it appears that the routing procedure did an adequate job of routing the flood waves. The major difference occurs at shallow depths just after the overbank elevations have been exceeded. The computed depths are noticeably larger than the observed depths in this range, especially for the floodplain section. This probably due to using a constant average n values in the equations. At shallow depths on the floodplain, the n values were much larger than the average value.

A problem relative to the unsteady flows was that there was very little attenuation of the flood wave because of the short test reach length used. The change in depth of the flood wave for

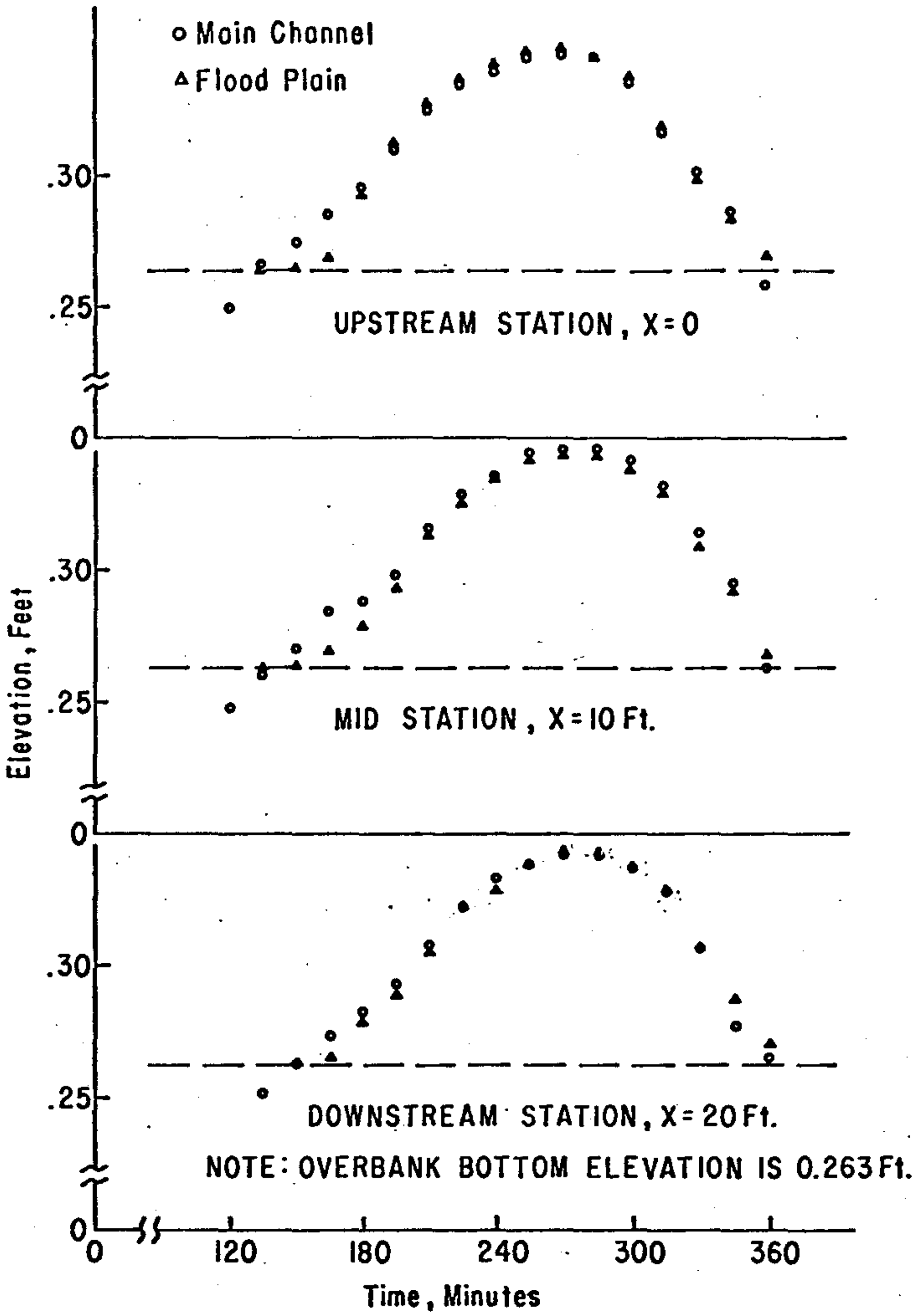

Figure 8 Observed water surface elevations for main channel and floodplain. Floodplain to main channel width ratio is 5.23, channel slope is 0.0022.

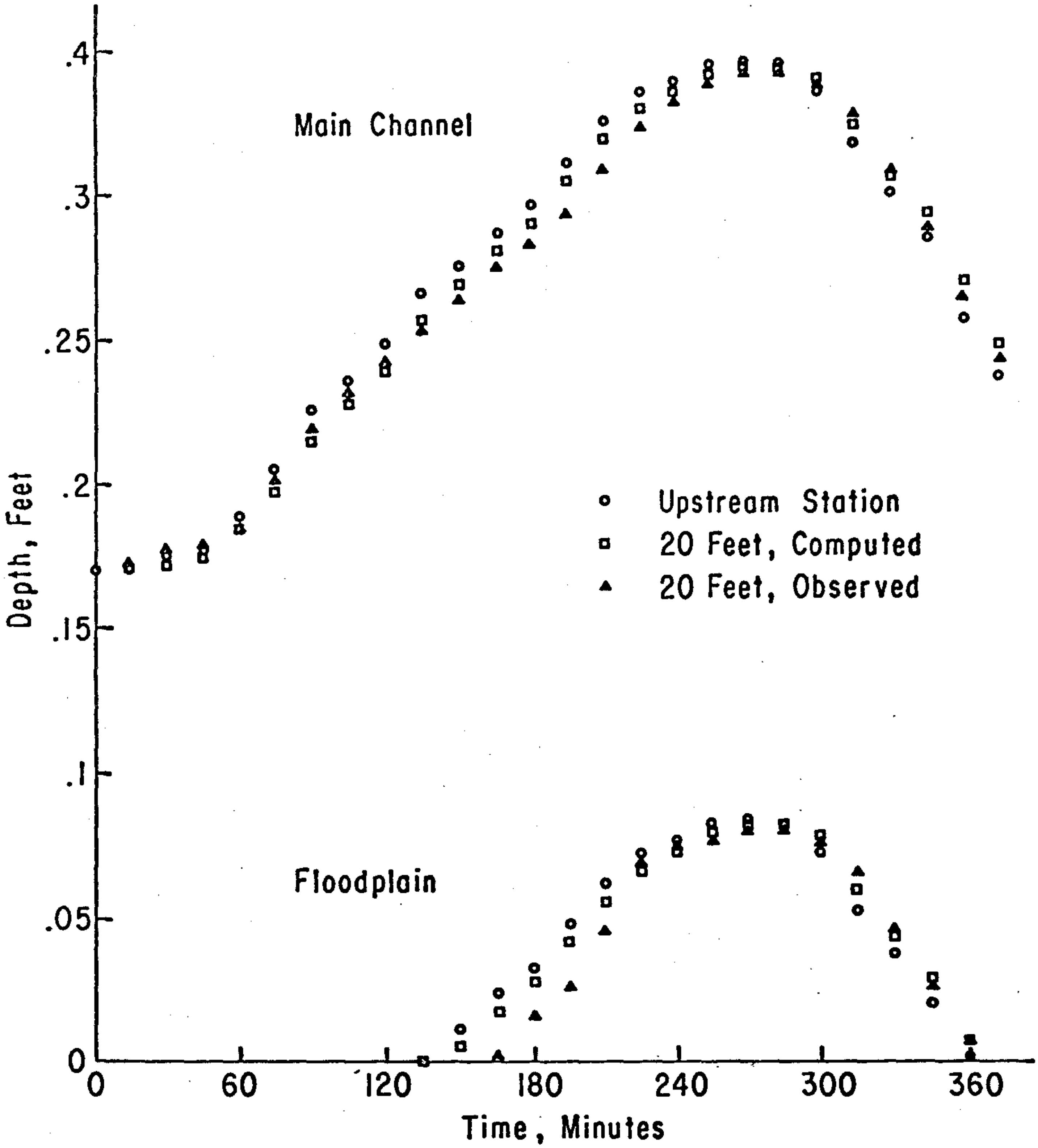

Figure 9 Depth hydrographs with roughness condition three. Floodplain to main channel width ratio is 5.23, channel slope is 0.0022.

the test reach length was of a magnitude about equal to the accuracy of the depth measuring equipment used. Thus, the unsteady flow data could not be analyzed and used to the extent that was desired.

Conclusions

1. The hydraulic radius as ordinarily computed in a regular channel results in erroneous discharge values for a combined channel in the depth range immediately above bank full stage of the main channel.

2. The floodplain flow appeared to have a significant retarding effect on the flow in the main channel.

3. The combined channel Manning Coefficient increased as the floodplain width increased relative to the main channel width.

4. The Manning Coefficient for the combined channel reflects the effect of channel geometry more than the effects of boundary roughness and slope.

5. As the floodplain width decreased, relative to the main channel width, the Manning Coefficients for the floodplain and main channel approached the same value at floodplain to main channel depth ratios greater than about 0.4.

6. The hydraulic radius and the wetted perimeter of the floodplain were greater with a divider separating the two section than without a divider for the same depth of flow in the main channel.

7. None of the methods commonly used to compute uniform flow discharge in a combined channel gave good results over the complete range of flow depths for the main channel-floodplain combination.

8. Except at very shallow floodplain depths, there was no difference in water surface elevation between the main channel and floodplain sections during the passage of a flood wave through the channel reach.

9. The forward and backward characteristic equations of the unsteady flow equations, solved using an explicit finite difference representation and a centered difference scheme, did an adequate job of routing the flood waves through the combined channel by breaking the combined channel into the main channel and floodplain sections and assuming a horizontal transverse water surface for the channel.

Publications

A paper is being prepared for publication in the Transactions of the American Society of Agricultural Engineers.

BIBLIOGRAPHY

1. Posey, J.C. "Computation of Discharge Including Over-Bank Flow." Civil Engineering-ASCE, Vol. 37, No. 4 (April, 1967), pp. 62-63.

2. Murphy, C.E. Similitude in Engineering. New York: The Ronald Press Company, 1950.